

# Minimal recipes for planetary cloudiness

George Datseris<sup>1</sup>, Joaquin Blanco<sup>2</sup>, Or Hadas<sup>3</sup>, Sadrine Bony<sup>4</sup>, Rodrigo Caballero<sup>2</sup>, Yohai Kaspi<sup>3</sup>, Bjorn Stevens<sup>4</sup>

<sup>1</sup>Max Planck Institute for Meteorology, Hamburg, Germany

<sup>2</sup>Department of Meteorology, Stockholm University, Stockholm, Sweden

<sup>3</sup>Department of Earth and Planetary Sciences, Weizmann Institute of Science, Rehovot, Israel

<sup>4</sup>Sorbonne University, LMD/IPSL, CNRS, Paris, France

## Key Points:

- Model fits are performed to the whole spatiotemporal observed cloudiness, using a minimal set of predictors and parameters
- Models capture global-mean, spatial variability, and mean seasonal cycle of both long and shortwave cloud radiative effects
- Cloud albedo is captured by a nonlinear combination of pressure velocity and inversion strength, while longwave effect is captured by temperature and pressure velocity, and variance of pressure velocity

---

Corresponding author: George Datseris, [george.datseris@mpimet.mpg.de](mailto:george.datseris@mpimet.mpg.de)

## Abstract

Clouds are primary modulators of Earth’s energy balance, in both short and longwave parts of the energy spectrum. It is thus important to understand the links connecting variabilities in cloudiness to variabilities in other state variables of the climate system, and also describe how these links would change in a changing climate. A conceptual model of planetary cloudiness can help elucidate these points. In this work we derive simple representations of cloudiness, that can be useful in creating a theory of planetary cloudiness. These representations illustrate how both spatial and temporal variability of cloudiness over the whole planet can be expressed in terms of basic state variables. Specifically, cloud albedo is captured by a nonlinear combination of pressure velocity and a measure of the temperature inversion, and cloud longwave effect is captured by surface temperature, pressure velocity, and standard deviation of pressure velocity. From these predictors, qualitative links may be drawn between equator-to-pole temperature gradients and cloudiness, which are relevant for an energy balance model. We conclude with a short discussion on the usefulness of this work in the context of global warming response studies.

## 1 Introduction

Clouds are one of the most fascinating, important, and complex components of Earth’s climate system. From the processes that start the cloud condensation nuclei on nanometer scales, to the cloud-circulation coupling on scales larger than megameters, clouds seem to be involved in all scales one would consider part of climate (Siebesma et al., 2020). Despite their importance, we seem to lack theoretical understanding of what controls planetary-wide cloudiness. For example, while we have a good understanding of the microphysics of cloud generation and radiative transfer through clouds (Houze, 2014; Cotton et al., 2014; Siebesma et al., 2020), it is difficult to use these theories to make claims about global cloudiness. Earth System Models (ESMs) and other bottom-up approaches do couple cloud formation to the global circulation. Unfortunately, so far they have not been proven effective in constraining global cloudiness variability (Sherwood et al., 2020; Zelinka et al., 2020). This makes it difficult to transparently establish links between variability in global cloudiness and Earth’s energy balance, or how this link would change in a changing climate.

Conceptual models could be useful in elucidating how the main features of cloudiness connect to the energy balance, and how these connections may respond to large scale climatic changes. However, existing conceptual work on cloudiness has focused on specific regions or regimes, such as the tropics (Pierrehumbert, 1995; Miller, 1997), the Walker circulation (Peters & Bretherton, 2005), or the formation of midlatitude storms (Charney, 1947; Eady, 1949; Pierrehumbert & Swanson, 1995), among others. What is missing, to our knowledge, is a conceptual framework that both closes the energy budget for a given climate state (and hence by necessity considers the planet as a whole), but also includes clouds. A suitable candidate for such a framework would be an energy balance model (Budyko, 1969; Sellers, 1969; Ghil, 1981; North & Kim, 2017) that explicitly represents dynamic cloudiness.

In this work we want to derive simple representations, or “recipes”, for planetary cloudiness, which can be potentially included in energy balance models, helping link variations in the energy budget and state variables of such models to variations in cloudiness and vice-versa. These representations therefore need to capture all main features of cloudiness, which are the global mean value, mean seasonal cycle, coarse spatial variability, and the difference between the shortwave and longwave impact of cloudiness. To derive representations that capture these features, we will use a quantitative top-down approach, where planetary cloudiness is directly decomposed into contributions from several simpler spatiotemporal fields. These fields are the “ingredients” of the recipe,

and in the rest of the text we will refer to them simply as predictors (in the sense of statistical predictors). The predictor contributions are calculated by fitting proposed models of predictors versus observed cloudiness. A model useful in theoretical work is one that can explain the most with the least amount of information, and therefore in this work the main objective is to derive minimal representations that use a few predictors. If the predictors used can be related to state variables represented in energy balance models, which are (typically) temperature and temperature differences, then cloudiness follows naturally from the representations that we will derive here.

Similar top-down approaches have been used frequently in the literature in the context of the empirical cloud controlling factors framework (Stevens & Brenguier, 2009). For tropical low clouds there are several studies summarized in the review by Klein et al. (2017), and see also Myers et al. (2021) for ESMs vs. observations. Attention has also been given to the midlatitude cloudiness (a summary of existing work on extratropical cloud controlling factors can be found in Kelleher and Grise (2019) and see also Grise and Kelleher (2021) for ESMs vs. observations). Our approach differs from past empirical approaches in that we fit absolute cloudiness, not anomalies, and we fit energetically meaningful cloudiness fields over all available space and time (see Sect. 2.3 for more details).

Section 2 describes our quantitative analysis, from defining cloudiness, which predictors to consider and why, how to fit predictor models on observed cloudiness, and how to judge the quality of the fits. Then, Sect. 3 presents the main analysis and results on how well the models capture cloud albedo and cloud longwave radiative effect. Section 3.4 shows that our models approximate CERES cloudiness better than using ERA5 radiation output directly. Section 3.5, discusses potential connections between the predictors used and equator-to-pole temperature gradients, setting the stage for future work on incorporating cloudiness in energy balance models. A summary and discussion of potential impact for sensitivity studies concludes the paper in Sect. 4.

## 2 Fitting planetary cloudiness

### 2.1 Quantifying cloudiness

To fit any model, a definition of cloudiness that is both quantitatively precise but also energetically meaningful is required. Hence, the radiative impact of cloudiness is targeted. For the shortwave part, we use the energetically consistent effective cloud albedo (in the following, just “cloud albedo”),  $C$ , estimated using the approach of Datsseris and Stevens (2021).  $C$  is a better way to quantify shortwave impact of cloudiness than the shortwave cloud radiative effect (CRE), because a large amount of variability of the latter actually comes from the variability of insolation (Datsseris & Stevens, 2021). For the longwave part the CRE,  $L$ , is a good representation of the radiative impact of clouds, and is a proxy for cloud effective emissivity which can be added in an energy balance model (e.g., Södergren et al. (2018)). Furthermore, it is not directly affected by the sun. Both  $C, L$  are derived from monthly averaged CERES EBAF data (Loeb et al., 2018) using 19 years of measurements (2001-2020).

### 2.2 Predictors considered

All predictors considered in this study are defined and listed in Table 1 and are obtained from monthly averaged ERA5 data (Hersbach et al., 2020) using 19 years of data (2001-2020). Pressure velocity  $\omega_{500}$ , estimated inversion strength  $EIS$ , surface wind speed  $V_{\text{sfc}}$ , sea surface temperature  $SST$ , and stratospheric specific humidity  $q_{700}$ , have been used numerous times in the literature and it is well understood that they play a role in controlling cloudiness.  $\omega_{500}$  is known to be important for both shortwave and longwave cloud radiative effects (Bony et al., 1997; Norris & Weaver, 2001; Bony et al., 2004; Nor-

ris & Iacobellis, 2005), and  $EIS$ ,  $V_{\text{sfc}}$ ,  $SST$ ,  $q_{700}$  have been used to fit cloud cover anomalies in a variety of regimes, see e.g., Klein et al. (2017); Kelleher and Grise (2019) and references therein for a more detailed discussion. Do note that the connections between predictors and cloudiness in the literature are exposed for specific regimes (such as tropical subsidence regions, or North midlatitudes, etc.), while here we will test their potential in fitting cloudiness over the whole planet.

Symbol	Description	Reference
$C$	Energetically consistent effective cloud albedo	Datseris and Stevens (2021)
$L$	Longwave cloud radiative effect	Loeb et al. (2018)
$\omega_{500}$	Pressure velocity at 500hPa	Grise and Kelleher (2021)
$\omega_{\text{std}}$	Standard deviation of $\omega_{500}$ within a month	Norris and Iacobellis (2005)
$\omega_{\text{up}}$	Fraction of updrafts of $\omega_{500}$ within a month	Bony et al. (1997)
$V_{\text{sfc}}$	10-meter wind speed	Brueck et al. (2015)
$SST$	Sea surface temperature (SST)	Qu et al. (2015)
$q_{\text{tot}}$	Total column water vapor	-
$q_{700}$	Specific humidity at 700hPa	Myers and Norris (2016)
$EIS$	Estimated inversion strength	Wood and Bretherton (2006)
$CTE$	Estimated cloud top entrainment index	Kawai et al. (2017)

**Table 1.** Fields to-be-predicted ( $C$ ,  $L$ ) and predictors considered in this study. An indicative reference for each is given as well. We multiple  $\omega_{500}$  with  $-1$  in this study, so that  $\omega_{500} > 0$  means upwards motion.

We included  $CTE$ , the estimated cloud top entrainment index, because Kawai et al. (2017) present it as an improvement over  $EIS$ , yet recent literature continues to use  $EIS$  instead of  $CTE$  (e.g., Grise and Kelleher (2021)), thus further analysis confirming whether  $CTE$  is indeed an improvement is necessary. Both  $q_{700}$ ,  $q_{\text{tot}}$  (with  $q_{\text{tot}}$  the total column water vapor) are a proxy for the moisture of an atmospheric column, and expected to be relevant when fitting  $L$ . In our analysis however,  $q_{700}$  gave consistently better fits when used in place of  $q_{\text{tot}}$ , keeping all other aspects fixed (not shown). This is likely why  $q_{\text{tot}}$  has not been used as a predictor in published literature and also why we will not discuss it more in the rest. Using  $q_{700}$  at 700hPa instead of  $q_{700}$  at surface results in only minor improvement of fit quality throughout the analysis (also not shown). The two uncommon predictors considered here that nevertheless have major positive impact on fit quality are standard deviation  $\omega_{\text{std}}$ , and fraction of updrafts  $\omega_{\text{up}}$ , of  $\omega_{500}$ . They are both derived from hourly  $\omega_{500}$  data, aggregated over monthly periods (we note that using up to 6-hourly sampled data yields little quantitative difference in  $\omega_{\text{std}}$ ,  $\omega_{\text{up}}$ ).

$\omega_{\text{up}}$  has been devised because we fit absolute values, not anomalies, see Sect. 2.3. Specifically in the case of  $C$ , we fit a quantity that is not only strictly positive, but further bounded in  $[0, 1]$ .  $\omega_{\text{up}}$  has the same property of being bounded to  $[0, 1]$ , while  $\omega_{500}$  has many negative values that may penalize the fitting process. Another advantage of  $\omega_{\text{up}}$  is that it can be used as a weight to distinguish between regions of large scale subsidence (in fact, this weighting aspect of  $\omega_{\text{up}}$  has already been used by Bony et al. (1997) to better understand the connection between CREs and SSTs in the tropics).

$\omega_{\text{std}}$ , which can be thought of as a simple quantifier of storminess, has been shown to be a useful predictor of cloudiness by Norris and Iacobellis (2005). There the authors highlighted the nonlinear connection between vertical motion and cloud generation (e.g., cloud optical depth increases more strongly with upward motion than it decreases with downwards motion). As we will discuss in more detail in Sect. 3.3, another argument fa-

voring  $\omega_{\text{std}}$  is that it relates cloudiness with the moisture of the air column much better than  $\omega_{500}$ .

### 2.3 Fitting process

Let  $Y$  be a measure of cloudiness ( $C$  or  $L$  from Sect. 2.1) and  $X_i$  be some predictor fields, for  $i = 1, \dots, n$ .  $Y, X_i$  are global spatiotemporal fields. We assume that with sufficient accuracy we can write

$$Y \approx M = f(X_1, \dots, X_n; p_1, \dots, p_m) \stackrel{\text{e.g.}}{=} p_1 X_1 + p_2 X_2 + p_3 X_1 X_2 \quad (1)$$

with  $p_j$ , for  $j = 1, \dots, m$  be some parameters to be estimated (all  $p_j \in \mathbb{R}$ ). In the following we will call  $f$  the “cloud fitting function”. Naturally, it is expected that different forms for  $f$  and/or sets of predictors will yield a better fit for  $C$  or  $L$  respectively, as each captures different aspects of cloudiness. Given a specific form for  $f$ , and a set of predictors  $X_i$ , the parameters  $p_j$  of the model are estimated via a standardized nonlinear least square optimization (Levenberg, 1944; Marquardt, 1963). The minimization objective is the squared distance between  $Y$  derived from CERES observations, and  $M$  produced by Eq. 1 by plugging into it predictors  $X_i$  from ERA5. All data have been transformed into an equal area grid of cell size  $\approx 250\text{km}$ , from their standard orthogonal longitude-latitude grids. Additionally, only data over ocean (a spatiotemporal mask is defined when CERES auxiliary ocean fraction is  $> 50\%$ ) are considered, as, favoring simplicity, we would like to derive minimal models that do not deal with the complexities of including a land type contribution. Data are limited to  $\pm 70^\circ$ , to avoid potential CERES measurement artifacts at the poles.

This approach of fitting models with free parameters to observed data is similar to the cloud controlling factors framework (CCFF), however there are some key differences. The first is that the data used here are not anomalies. This means that the mean value of  $Y$ , and its seasonal cycle, must be captured by the fit. Consequently, if all predictors are zero, then total cloudiness must also be zero. The importance of capturing the mean value and mean seasonal cycle is further enforced by the fact that the inter-annual variability of cloudiness is small in decadal timescales (Stevens & Schwartz, 2012; Stephens et al., 2015) and hence the mean seasonal cycle captures the majority of the signal (e.g., for hemispherically averaged all-sky reflected shortwave radiation, 99% of the variability (Datseris & Stevens, 2021)). Since the cloud fitting function is expected to capture the mean, it can be a nonlinear function (and if it is linear, then it must have intercept 0 by force). Another argument behind allowing nonlinear functions is that, generally speaking, a theory of cloudiness could answer “how cloudy is it” in fundamentally different climatic states, not just small deviations from a reference climate (which justifies using a linear framework).

A second difference with typical CCFF studies is that we fit across all available space and time without any restrictions to special regions of space or cloud types. Typically in CCFF the fitted parameters (which are linear coefficients) are either aggregated over some specific region of Earth (e.g., subtropical subsidence regions like in Myers and Norris (2016)), or are fitted for each spatial point of the planet (e.g., like in Grise and Kelleher (2021)), or the focus is exclusively on a specific cloud type (e.g., low clouds like in Myers et al. (2021)).

### 2.4 Quantitatively measuring fit quality

It is important to be able to quantify fit quality with an objective measure that is independent of what predictors are used, how they are combined, or even whether the fit is over  $C$  or  $L$ . A common choice for such tasks is the normalized root mean square

error (NRMSE), defined as

$$\epsilon(Y, M) = \sqrt{\frac{\sum_n (Y_n - M_n)^2}{\sum_n (Y_n - \bar{Y})^2}} \quad (2)$$

with  $Y, M$  as in Eq. 1,  $\bar{Y}$  the mean of  $Y$  and  $n$  enumerates the data points. This error measure is used routinely in e.g., spatiotemporal timeseries prediction (Isensee et al., 2019), and is a statistic agnostic of the values of  $Y, M$  that can compare fit quality across different ways of fitting or different input data. If  $e > 1$  the mean value of  $Y$  is a better model than  $M$  (equivalently, the variance of the observations is smaller than the mean square error between fit and observations). Do note however, that there several ways to compute  $\epsilon$ : on full spatiotemporal data, on zonally and temporally averaged data, or on the seasonal cycles of tropics ( $0^\circ$ - $30^\circ$  degrees) and midlatitudes ( $30^\circ$ - $70^\circ$  degrees). In addition, one can also use the Pearson correlation coefficient between the timeseries of  $Y, M$ , computed at each spatial location and then averaged over space. Each measure highlights a different aspect of fit quality (e.g., capturing spatial or temporal variability well). All measures were taken into account when deciding the best fits (see below).

### 3 Results & Discussion

In this section we describe the fit results, starting with the simplest scenario, that can serve as guidance for the followup analysis, and then presenting the “best” fits for cloud albedo  $C$  and longwave cloud radiative effect  $L$ . To clarify, “best” does not mean the fits with least possible  $\epsilon$  out of all conceivable combinations of predictors and cloud fitting functions  $f$ . As already discussed in the introduction, a main goal of this work is to pave the way for representing cloudiness in a conceptual energy balance model. Therefore, the “best” fits are the simplest, most minimal fits, that accommodate intuitive physical justification, but also provide good fit quality (i.e., low values for  $\epsilon$ ). Only the requirement is small error  $e$  is objective, while the rest have at least partly a subjective nature. Additionally, fits that use simpler predictors, that can be more straightforwardly represented in a conceptual framework, are preferred. If two fits have approximately equal error  $\epsilon$ , but one uses a simpler predictor (e.g., surface temperature  $SST$  versus atmospheric specific humidity  $q_{700}$ ), the first fit is “better”. Certainly, slightly different variations on the exact form  $f$  and predictors used could yield similar versions of a “best fit”, but these small variations are not crucial for the scope of this work.

#### 3.1 Two predictor linear model

The simplest model one can use for the cloud fitting function  $f$  is one that has two predictors and two free parameters in a linear manner:  $f = p_1 X_1 + p_2 X_2$ . Even if this model does not yield a good fit for cloudiness, it is advantageous to start with it nevertheless. All possible linear combinations given all possible predictors of Sect. 2.2 are only 36, and they can already highlight which predictors are worth a closer look for which measure of cloudiness. The results are in Fig. 1, which showcases two different error measures (error in temporally and zonally mean cloudiness, and error in mean seasonal cycle of cloudiness), and how these errors depend on which predictors are used for the linear fit.

The majority of combinations result in low fit quality ( $e \geq 0.9$ ). Nevertheless, Fig. 1 reveals some useful information. For  $C$ , a measure of the inversion strength is necessary for a decent fit and the combination of  $\omega_{\text{up}}$  and  $CTE$  result in the best case scenario. For  $L$ , the most important predictor seems to be  $\omega_{\text{std}}$ , which gives decent fits in both space and time for a wide selection of second predictors (while  $\omega_{500}$  gives decent fits only in time). A second important predictor for  $L$  seems to be  $q_{700}$  or  $SST$ .

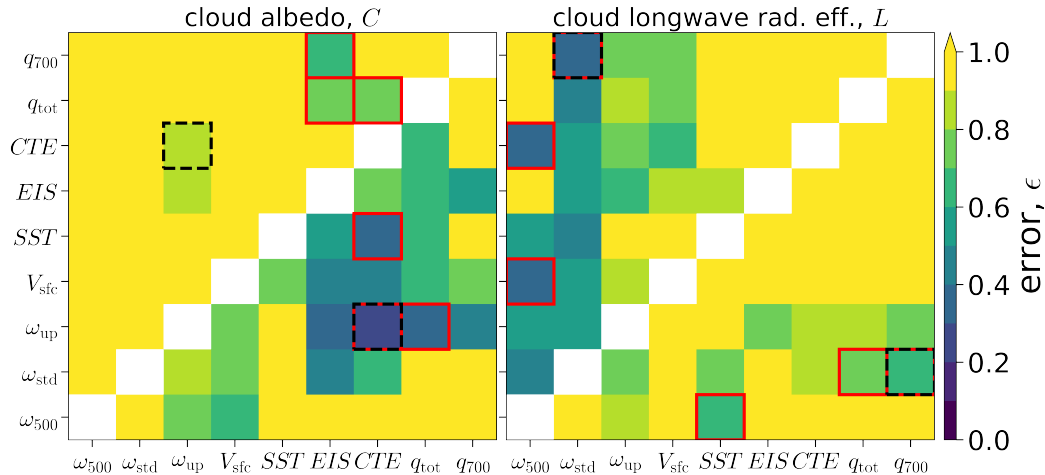


**Figure 1.** Error in temporally and zonally mean cloudiness (lower-right triangle of heatmap), and error in mean seasonal cycle (upper-left triangle of heatmap), as a function of which predictors of the x and y axis combine into a linear model  $f = p_1 X_1 + p_2 X_2$  for fitting cloud albedo (left plot) or longwave cloud radiative effect (right plot). Red outline highlights the three combinations with the lowest error in each category, while black dashed outline highlights the combination with lowest error overall (by multiplying the two different error measures). It is possible that  $e > 1$  because we are fitting without intercept.

### 3.2 Best fit for cloud albedo $C$

While it is already clear in the literature that  $\omega_{500}$  is an important predictor for shortwave impact of clouds (Sect. 2.2), the fact that  $\omega_{\text{up}}$  performs so much better in a linear model hints that the bounded nature of albedo,  $C \in [0, 1]$ , is important. Negative predictor values yield low fit quality and also penalize fitting well positive values. One way to counter this would be to use  $\omega_{\text{up}}$  as probability weight multiplying other predictors. An alternative would be to use appropriate nonlinear functions of the more basic  $\omega_{500}$ . Regardless the choice,  $CTE$  must also be included in the model, as it is necessary to capture the important contribution of low clouds.

A model that satisfies all these requirements, and achieves the best fit, is

$$C = 50p_1 (\tanh(p_2\omega_{500} + p_3CTE) + 1) \quad (3)$$

where we used the nonlinear function  $x \rightarrow (\tanh(x)+1)/2$  to map predictors into  $[0, 1]$  space (the prefactor  $50=100/2$  simply makes the equation measured in % units). The results of the fit (i.e., estimating the parameters  $p_1, p_2, p_3$  that give least square error between Eq. 3 and the observed CERES  $C$ ) are in Fig. 2. The model fit captures all main features of cloud albedo (including its mean value), and achieves  $e = 0.54$  over the full space and time,  $e = 0.19$  in the zonal and temporal average, and  $e = 0.65$  in mean seasonal cycle. The inclusion of the parameter  $p_1$  is necessary, because in observations cloud albedo does not saturate to 1, but to much lower values (see Fig. 2). We also note that using  $EIS$  instead of  $CTE$  in the model decreases fit quality significantly, because, while  $EIS$  and  $CTE$  both capture subtropical low cloud albedo well, only  $CTE$  also captures midlatitude low cloud albedo well, while  $EIS$  mostly fails.

Adding more predictors increases fit quality only slightly. E.g., adding a factor  $p_4 V_{\text{sf}}$  inside the tanh function decreases time and zonal mean error to  $e = 0.18$  from  $e = 0.19$

and seasonal cycle error to  $e = 0.6$  from  $e = 0.65$ , as well as captures hemispheric asymmetries in  $C$  slightly better. That the decrease in error is so small gives confidence that that the basic physics governing cloud albedo are already captured by Eq. 3. Further fine-tuning of the model only captures higher order details that will likely not be included in a conceptual theory anyway.

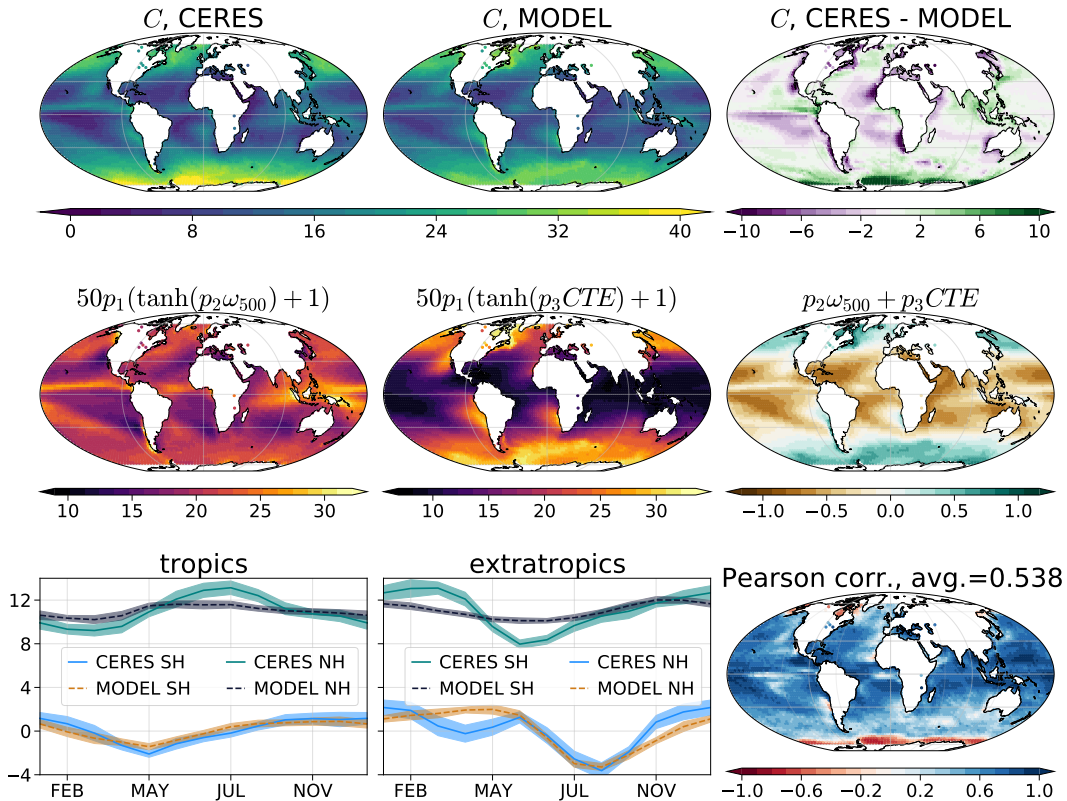


**Figure 2.** Results of fitting cloud albedo  $C$  (units of %) with the simple model of Eq. 3. First row are time-averaged maps of the observed data, the fit, and a difference between them. See also Fig. 4 for a zonally averaged version. Second row are the contributions of different terms in the model. Third row shows how well the model captures temporal variability. First two panels are the mean seasonal cycles (with semi-transparent bands noting the standard deviation around each month) in the tropics ( $0-30^\circ$ ) and extratropics ( $30-70^\circ$ ). The mean value of all cycles has been subtracted, and SH cycles are offset for visual clarity. The third panel is a map of the Pearson linear correlation coefficient between the timeseries of the model and CERES data at each grid point. Units of  $\omega_{500}$  in Pa/s and  $CTE$  in K, and  $p_1 = 0.4$ ,  $p_2 = 6.87$ ,  $p_3 = 0.08$ . Note that we multiply  $\omega_{500}$  with  $-1$  before any analysis (so that  $\omega_{500} > 0$  means updrafts).

Since Eq. 3 is nonlinear, it is not trivial to disentangle the contribution of the individual predictors. The middle row of Fig. 2 provides some insights. Both  $CTE$  and  $\omega_{500}$  contribute to midlatitude cloud albedo, but  $CTE$  slightly more so. In the tropics  $\omega_{500}$  contributes the albedo of the convective regimes (ITCZ, Maritime Continent), and  $CTE$  the albedo of the low stratocumulus decks (subsidence regions).  $CTE$  is in some sense a more important predictor than  $\omega_{500}$ , because if we set explicitly  $p_2 = 0$  in Eq. 3, we get lower error of  $e = 0.7$  in full space and time, versus the error of  $e = 0.9$  we would get if we set explicitly  $p_3 = 0$  instead. Alternative models to Eq. 3 can give qualita-

tively same results using  $\omega_{\text{up}}$  instead of  $\omega_{500}$ . For example, using  $f = p_1\omega_{\text{up}} + p_2CTE \times (1 - \omega_{\text{up}})$  provides similar, but slightly worse, fit quality with  $e = 0.57$  over full space and time and  $e = 0.23$  over time and zonal mean. However,  $\omega_{500}$  is a simpler predictor than  $\omega_{\text{up}}$ , and hence a model with  $\omega_{500}$  is more minimal (and thus, “better”).

Of course, there are some discrepancies between model and observations. The most notable ones are:

1. Southern ocean cloud albedo is not as high as in CERES. Generally, the model fit is more symmetric in its midlatitude cloud albedo, while CERES has strong asymmetry with SH having much higher albedo (Datsiris & Stevens, 2021).
2. There are overall large errors near most coasts. This is expected, because we have set up a fit only over ocean.
3. In CERES, the albedo of the West Atlantic and Central Pacific ocean regions directly west of the subtropical stratocumulus decks is nearly 0. In the model fit, the albedo there is significantly higher, up to 6 units more. This stems from  $\omega_{500}$ .
4. The temporal variability in the SH midlatitudes is captured poorly by the model as seen both in the seasonal cycles but also in the (incorrect) anti-correlation near the shores of Antarctica. We believe this is because of the co-variability with ice affecting cloud albedo (and perhaps even making CERES measurements attribute larger-than-normal albedo to clouds), but surface type variations are not considered in our model.

### 3.3 Best fit for longwave cloud radiative effect $L$

Fitting  $L$  is more complex, versus fitting  $C$ , for mainly two reasons. First, the longwave effect of a cloud depends strongly on the infrared opacity, and hence moisture content, of the atmospheric column overshadowed by the cloud. Moisture content though is, at least partly, controlled by temperature. Warm and humid atmospheres are already almost opaque to longwave radiation, and hence the presence of a cloud would have little difference. Contrariwise, in a cold and dry atmosphere a cloud would bring a lot of extra absorption of outgoing longwave radiation and hence large  $L$ . A second reason that makes  $L$  a harder quantity to fit versus  $C$  is that cloud height matters a lot for its effective emissivity (as cloud height sets its temperature), while cloud height does not have a significant effect on cloud albedo (keeping all other factors fixed).

It is perhaps for these reasons that we were not able to find a model that had as good of a fit for  $L$  as it had for  $C$  when restricting the model to using at most two predictors. After an analysis of several different linear and nonlinear combinations, the “best” model we concluded in is

$$L = p_1\omega_{\text{std}} + p_2\omega_{500} + p_3SST. \quad (4)$$

The results of the fit are in Fig. 3. Similarly with  $C$ , the fit captures all main features of  $L$  modulo some deficiencies listed below. The fit errors are  $e = 0.63$  over full space and time,  $e = 0.46$  in time and zonal mean and  $e = 0.41$  in mean seasonal cycle. Spatial variability is captured worse for  $L$  versus  $C$ , but temporal variability is captured better for  $L$  versus  $C$ . A factor that contributes to this is that the temporal variability of  $L$  is much simpler versus  $C$  (e.g., relative power of 12-month periodic component is much larger in  $L$  timeseries, leading to simpler seasonal cycle temporal structure, compare last rows of Figs. 2 and Figs. 3).

Before discussing the main discrepancies between fit and observation, let us first justify the choice of predictors. Monthly-mean  $\omega_{500}$  is a proxy to cloud height (persistent updrafts and with larger magnitude should result in higher clouds). The surface temperature  $SST$  is a proxy for the emissivity of the air column without a cloud, because the potential total moisture content of atmospheric columns is a monotonically increasing function of temperature under first approximation. Using  $q_{700}$ , specific humidity at

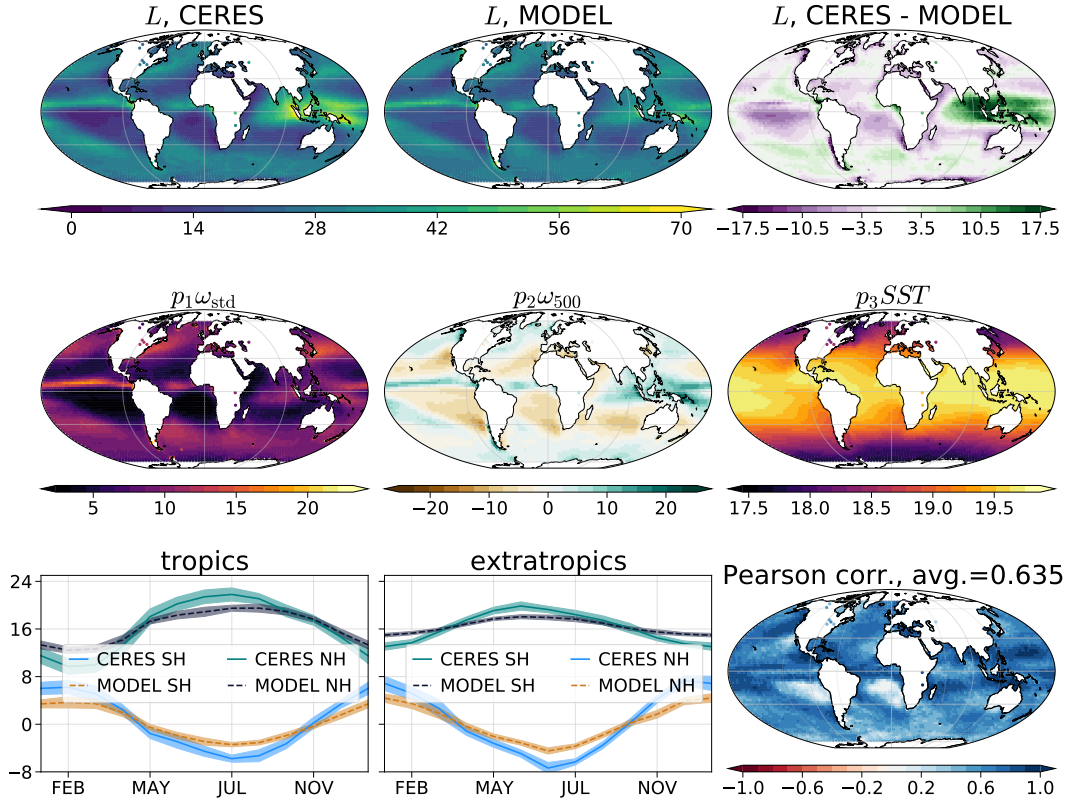


**Figure 3.** As in Figure 2 but now for longwave cloud radiative effect  $L$ . Units of  $L$  in  $\text{W}/\text{m}^2$ ,  $\omega_{500}, \omega_{\text{std}}$  in  $\text{Pa}/\text{s}$ ,  $SST$  in  $\text{K}$ , and  $p_1 = 42.68, p_2 = 208.9, p_3 = 0.06558$ .

700hPa instead of  $SST$ , yields worse capturing of spatial variability (with  $e = 0.6$  versus  $e = 0.46$  in time and zonal mean) but improves even more the capturing of temporal variability (with  $e = 0.34$  versus  $e = 0.41$  in mean seasonal cycle). Given that  $SST$  is a more basic predictor than  $q_{700}$ , and is directly represented in conceptual energy balance models,  $SST$  is preferred. Furthermore, and as was the case with  $C$ , adding more predictors, or additional nonlinear terms of existing predictors, increases fit quality but only slightly. E.g., an additional nonlinear factor  $p_4 \omega_{\text{std}} \times SST$  decreases the zonal and temporal mean error from  $e = 0.46$  to  $e = 0.43$ , but this small change does not justify the increase of complexity of adding a fourth free parameter to be tuned, even though we remain at three individual predictors (we remind that the “minimality” of the fit is a bigger requirement than its error minimization).

Interestingly,  $\omega_{\text{std}}$  is the most important predictor for  $L$ . Even though  $\omega_{500}$  captures a broader range of values ( $\sim 40$  versus the  $\sim 30$  of  $\omega_{\text{std}}$ ), absence of  $\omega_{\text{std}}$  significantly lowers fit quality in all combinations of cloud fitting functions  $f$  and predictors we tested, even when including  $\omega_{500}$  in all of them. The spatial structure of  $\omega_{\text{std}}$  is the most similar to the spatial structure of  $L$ , with the main difference being that for  $\omega_{\text{std}}$  the peak values in tropics and extratropics have equal magnitude, while for  $L$  the tropic peak values have 33% more magnitude. Hence, some other predictor must lower the extratropical magnitude of  $\omega_{\text{std}}$ , and here this role is fulfilled by  $SST$  in Eq. 4 (or  $q_{700}$ , if one uses it instead of  $SST$ ).

A physical connection between  $\omega_{\text{std}}$  with  $L$  can be thought as follows: persistent updrafts, that are captured by  $\omega_{500}$ , would lead to a moist atmosphere and hence weak

$L$ , mostly irrespectively of cloud height. On the other hand, consistent pumping of air up and down (high  $\omega_{\text{std}}$ , but almost zero  $\omega_{500}$ ) would leave the atmosphere dry (for at least half the time), but the formed clouds would linger longer above the dry atmosphere and have a disproportionately strong effect, yielding high  $L$ . In the midlatitudes both  $L$  and  $\omega_{\text{std}}$  have their latitudinal maximum in the middle of the Ferrel cell (40-45°), where  $\omega_{500} \approx 0$ . Of course, monthly-mean  $\omega_{500} \approx 0$ , but in the hourly timescale there is a lot of vertical motion, as captured by the high values of  $\omega_{\text{std}}$ . This reflects the fact that storms form in the middle of the Ferrel cell, not its end. In the tropics,  $\omega_{500}$  and  $\omega_{\text{std}}$  have little differences in their latitudinal structure.

The most noteworthy discrepancies between fit and observations are:

1.  $L$  of Maritime Continent is largely underestimated by the model. This mainly stems from  $\omega_{\text{std}}$  having relatively smaller values there versus e.g., ITCZ.
2. For same reason as above,  $L$  of ITCZ is slightly overestimated in the fit.
3. Similarly with  $C$ , the difference between the high  $L$  of (e.g.,) ITCZ and the  $\approx 0$   $L$  of the ocean regions in West Atlantic and Central Pacific is not as sharp in the model as in CERES.
4. While the temporal structure (i.e., the relative power of regular 12- and 6-month periodic components) of the seasonal cycles is captured well, the total magnitude of the cycles is consistently smaller in the fit than in observations. Using  $q_{700}$  instead of  $SST$  as second predictor removes this deficiency.

### 3.4 Comparison with ERA5 and reduced data

For obtaining reference values of the errors we report here, we also compare the outcome of our analysis with using direct ERA5 radiation output to measure  $C$  or  $L$ . Calculating  $L$  is straightforward, however, we cannot compute the energetically consistent effective cloud albedo from ERA5, because it requires cloud optical depth, a field not exported by ERA5. Instead, we can compute the cloud contribution to atmospheric albedo  $\alpha^{\text{CLD}}$  (specifically, Eq. 3 from Datsersis and Stevens (2021)), which has only small differences with  $C$ .  $\alpha^{\text{CLD}}$  also has the downside of not having a time dimension due to absence of sunlight for large portions of the data (see discussion in Datsersis and Stevens (2021) for more details).

We also present fits and their errors for fitting reduced data directly, specifically temporally and zonally averaged data. Fitting reduced data can only increase fit quality, because this case neglects higher-order effects that contribute to e.g. zonal or temporal structure, but are averaged out in the reduced version. If, however, the fit quality increases only slightly, that gives confidence that the basic connections captured by our models are indeed the most important ones and hence also dominate full spatiotemporal variability. The results are in Fig. 4.

Two conclusions can be readily drawn: (1) our fits are have smaller error  $\epsilon$  than using direct ERA5 radiation output, (2) fitting the simplified version of temporally and zonally averaged data increases fit quality only slightly, further validating the fit quality.

### 3.5 Potential connection with energy balance models

In the introduction we discussed the benefits of including cloudiness in an energy balance model. There are two steps in achieving this in practice. First, express cloudiness as a function of simpler physical quantities. Second, represent these quantities in an energy balance model. In this work we achieved the first step. To accomplish the second step, one would have to express predictors  $\omega_{500}, \omega_{\text{std}}, CTE$  as functions of temperature, or temperature differences (which are the typical state variables of energy balance

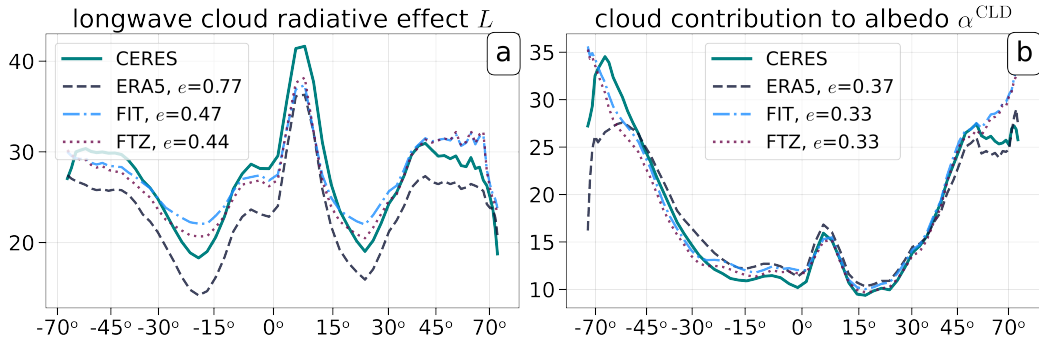


**Figure 4.** Temporally and zonally averaged data (and their errors  $e$ , Eq. 2, versus the CERES curve) of CERES, our model fits, and direct ERA5 output for (a) the longwave cloud radiative effect  $L$  and (b) the cloud contribution to atmospheric albedo  $\alpha^{\text{CLD}}$ . In (a), “FIT” is over all space and time, and “FTZ” is a fit over temporally and zonally averaged data. In (b), “FIT” is a fit over temporally averaged data (no time information can be used), and “FTZ” is as before.

models). While this task is certainly a subject of future research on its own right, the choice of predictors was such that there are physically sensible qualitative connections to start from.

The theory behind the baroclinic instability (Charney, 1947; Eady, 1949; Pierrehumbert & Swanson, 1995) states that midlatitude storms are driven by the equator-to-pole temperature gradient. Hence, larger temperature gradient would lead to stronger storms, reflected by a larger  $\omega_{\text{std}}$  in the midlatitudes. The mean circulation in the Ferrel cell (represented by  $\omega_{500}$ ) will likely also increase due to continuity and the increased momentum carried by the storms. In the tropics, the Held-Hou model (Held & Hou, 1980) establishes a proportionality between the strength of the Hadley circulation  $\omega_{500}$  and gradients in insolation, which, in a first approximation, can be taken as gradients in temperature. We have noticed that in the tropics the spatial structure of  $\omega_{500}$  and  $\omega_{\text{std}}$  are very similar, but why this is the case is not immediately clear from the Held-Hou model.

The estimated cloud top entrainment index  $CTE$  is harder to express in terms of temperatures. Measures like  $CTE$  (or  $EIS$  or the Lower Stratospheric Stability) capture the temperature inversion magnitude between the boundary layer and surface (Wood & Bretherton, 2006). In the tropical subsidence regions, this inversion strength can be conceptually tied to temperature gradient between the warm equator and colder ocean of subtropics as follows: The free tropospheric temperature is, to a first approximation, homogenized by gravity waves to the value in the convecting regions (weak temperature gradient approximation (Sobel et al., 2001)). Surface temperature in the tropical subsidence regions however reflects the colder ocean temperature. The connection of  $EIS$  with the underlying ocean temperature in the case of midlatitudes is less clear. Conceptually, a temperature inversion can occur in cyclonic storms due to mechanical reasons: warm air masses from the midlatitudes are forced on top of the cold polar fronts, creating a temperature inversion scenario. However, more research on the subject is necessary to make more concrete claims.

Given these considerations, it seems that a promising way to express these predictors (and hence cloudiness) in an energy balance model is via the equator-to-pole temperature gradient. Future research should focus in validating this claim in more detail, but also make the qualitative connections we drew here quantitative and with clear functional forms.

## 4 Conclusions

The goal of this work was to identify ways one can accurately represent observed planetary cloudiness using as few and as simple components as possible, such as surface temperature or vertical wind speed. We have shown that the combination of pressure velocity  $\omega_{500}$  and a measure of temperature inversion  $CTE$  are enough to capture all main features of cloud albedo, while surface temperature  $SST$ , standard deviation of hourly pressure velocity  $\omega_{std}$ , and  $\omega_{500}$ , capture all main features of longwave cloud radiative effect. Qualitatively, these predictors can be connected with equator-to-pole temperature gradients and future research can should strive to make these qualitative connections quantitative.

Equations 3 and 4, and the analysis of Sect. 3, can also be used to quantify the response of cloudiness to a change in the climate system. For example, how would a change in the variability of the circulation or inversion strength impact global cloudiness and hence the energy balance. But also, the equations can provide spatially localized information on such changes, such as in which areas of the globe would circulation changes impact global cloudiness the most. These applications seem useful for e.g., better quantifying cloud sensitivities in the context of global warming. However, we must be aware that the exact parameter values  $p_j$  in Eqs. 3 and 4 have been derived from fitting on current climate (spanning two decades). At the moment we do not have any guarantee that their values would be the same in a significantly different climate, and one would need to perform a similar analysis as here to further confirm this.

## Acknowledgments

We thank Hauke Schmidt for helpful scientific discussions on this work. The datasets used in this study are monthly mean CERES EBAF (Loeb et al., 2018; Kato et al., 2018; Doelling et al., 2013; Rutan et al., 2015) for surface & top of the atmosphere radiation fields, and cloud properties, monthly mean ERA5 (Hersbach et al., 2020) for temperature, pressure, humidity, and hourly mean ERA5 for pressure velocity. All data are available for download online. The code base that performed the analysis of this paper, including the generation of all figures, is also available online (Datseris, 2022). The code can also be used to fit any arbitrary spatiotemporal field with any combination of functional forms and predictor fields.

**Author contributions.** G.D. performed the primary analysis and wrote the first draft. All authors contributed key ideas that shaped the study, and helped revise the draft.

## References

- Bony, S., Dufresne, J.-L., Treut, H. L., Morcrette, J.-J., & Senior, C. (2004, March). On dynamic and thermodynamic components of cloud changes. *Climate Dynamics*, 22(2-3), 71–86. Retrieved from <https://doi.org/10.1007/s00382-003-0369-6> doi: 10.1007/s00382-003-0369-6
- Bony, S., Lau, K.-M., & Sud, Y. C. (1997). Sea surface temperature and large-scale circulation influences on tropical greenhouse effect and cloud radiative forcing. *Journal of Climate*, 10(8), 2055 - 2077. Retrieved from [https://journals.ametsoc.org/view/journals/clim/10/8/1520-0442\\_1997\\_010\\_2055\\_sstals\\_2.0.co\\_2.xml](https://journals.ametsoc.org/view/journals/clim/10/8/1520-0442_1997_010_2055_sstals_2.0.co_2.xml) doi: 10.1175/1520-0442(1997)010<2055:SSTALS>2.0.CO;2
- Brueck, M., Nuijens, L., & Stevens, B. (2015, March). On the seasonal and synoptic time-scale variability of the north atlantic trade wind region and its low-level clouds. *Journal of the Atmospheric Sciences*, 72(4), 1428–1446. Retrieved from <https://doi.org/10.1175/jas-d-14-0054.1> doi: 10.1175/jas-d-14-0054.1
- Budyko, M. I. (1969). The effect of solar radiation variations on the climate of the

- Earth. *Tellus*, 21(5), 611–619. doi: 10.3402/tellusa.v21i5.10109
- Charney, J. G. (1947, oct). The dynamics of long waves in a baroclinic westerly current. *Journal of the Atmospheric Sciences*, 4(5), 136–162. Retrieved from [http://journals.ametsoc.org/doi/10.1175/1520-0469\(1947\)004%3C0136:TDOLWI%3E2.0.CO;2](http://journals.ametsoc.org/doi/10.1175/1520-0469(1947)004%3C0136:TDOLWI%3E2.0.CO;2) doi: 10.1175/1520-0469(1947)004<0136:TDOLWI>2.0.CO;2
- Cotton, W. R., Bryan, G., & Van Den Heever, S. C. (2014). *Storm and cloud dynamics* (2nd ed.). Academic Press.
- Datseris, G. (2022). *Code for the paper “minimalistic fits to planetary cloudiness”*. Zenodo. doi: 10.5281/zenodo.6336045
- Datseris, G., & Stevens, B. (2021, August). Earth’s albedo and its symmetry. *AGU Advances*, 2(3). Retrieved from <https://doi.org/10.1029/2021av000440> doi: 10.1029/2021av000440
- Doelling, D. R., Loeb, N. G., Keyes, D. F., Nordeen, M. L., Morstad, D., Nguyen, C., ... Sun, M. (2013, June). Geostationary enhanced temporal interpolation for CERES flux products. *Journal of Atmospheric and Oceanic Technology*, 30(6), 1072–1090. Retrieved from <https://doi.org/10.1175/jtech-d-12-00136.1> doi: 10.1175/jtech-d-12-00136.1
- Eady, E. T. (1949). Long waves and cyclone waves. *Tellus*, 1(3), 33–52.
- Ghil, M. (1981). Energy-Balance Models: An Introduction. In *Climatic variations and variability: Facts and theories* (pp. 461–480). Dordrecht: Springer Netherlands. Retrieved from [http://link.springer.com/10.1007/978-94-009-8514-8\\_27](http://link.springer.com/10.1007/978-94-009-8514-8_27) doi: 10.1007/978-94-009-8514-8\_27
- Grise, K. M., & Kelleher, M. K. (2021). Midlatitude cloud radiative effect sensitivity to cloud controlling factors in observations and models: Relationship with southern hemisphere jet shifts and climate sensitivity. *Journal of Climate*, 34(14), 5869–5886. doi: 10.1175/JCLI-D-20-0986.1
- Held, I. M., & Hou, A. Y. (1980, March). Nonlinear axially symmetric circulations in a nearly inviscid atmosphere. *Journal of the Atmospheric Sciences*, 37(3), 515–533. Retrieved from [https://doi.org/10.1175/1520-0469\(1980\)037<0515:nascia>2.0.co;2](https://doi.org/10.1175/1520-0469(1980)037<0515:nascia>2.0.co;2) doi: 10.1175/1520-0469(1980)037<0515:nascia>2.0.co;2
- Hersbach, H., Bell, B., Berrisford, P., Hirahara, S., Horányi, A., Muñoz-Sabater, J., ... Thépaut, J.-N. (2020, June). The ERA5 global reanalysis. *Quarterly Journal of the Royal Meteorological Society*, 146(730), 1999–2049. Retrieved from <https://doi.org/10.1002/qj.3803> doi: 10.1002/qj.3803
- Houze, R. A., Jr. (2014). *Cloud dynamics* (2nd ed.). Academic Press.
- Isensee, J., Datseris, G., & Parlitz, U. (2019, October). Predicting spatio-temporal time series using dimension reduced local states. *Journal of Nonlinear Science*, 30(3), 713–735. Retrieved from <https://doi.org/10.1007/s00332-019-09588-7> doi: 10.1007/s00332-019-09588-7
- Kato, S., Rose, F. G., Rutan, D. A., Thorsen, T. J., Loeb, N. G., Doelling, D. R., ... Ham, S.-H. (2018, May). Surface irradiances of edition 4.0 clouds and the earth’s radiant energy system (CERES) energy balanced and filled (EBAF) data product. *Journal of Climate*, 31(11), 4501–4527. Retrieved from <https://doi.org/10.1175/jcli-d-17-0523.1> doi: 10.1175/jcli-d-17-0523.1
- Kawai, H., Koshiro, T., & Webb, M. J. (2017, November). Interpretation of factors controlling low cloud cover and low cloud feedback using a unified predictive index. *Journal of Climate*, 30(22), 9119–9131. Retrieved from <https://doi.org/10.1175/jcli-d-16-0825.1> doi: 10.1175/jcli-d-16-0825.1
- Kelleher, M. K., & Grise, K. M. (2019). Examining Southern Ocean cloud controlling factors on daily time scales and their connections to midlatitude weather systems. *Journal of Climate*, 32(16), 5145–5160. doi: 10.1175/JCLI-D-18-0840.1
- Klein, S. A., Hall, A., Norris, J. R., & Pincus, R. (2017). Low-Cloud Feedbacks

- from Cloud-Controlling Factors: A Review. *Surveys in Geophysics*, 38(6), 1307–1329. doi: 10.1007/s10712-017-9433-3
- Levenberg, K. (1944). A method for the solution of certain non-linear problems in least squares. *Quarterly of Applied Mathematics*, 2(2), 164–168. Retrieved from <https://doi.org/10.1090/qam/10666> doi: 10.1090/qam/10666
- Loeb, N. G., Doelling, D. R., Wang, H., Su, W., Nguyen, C., Corbett, J. G., ... Kato, S. (2018, January). Clouds and the earth’s radiant energy system (CERES) energy balanced and filled (EBAF) top-of-atmosphere (TOA) edition-4.0 data product. *Journal of Climate*, 31(2), 895–918. Retrieved from <https://doi.org/10.1175/jcli-d-17-0208.1> doi: 10.1175/jcli-d-17-0208.1
- Marquardt, D. W. (1963, June). An algorithm for least-squares estimation of non-linear parameters. *Journal of the Society for Industrial and Applied Mathematics*, 11(2), 431–441. Retrieved from <https://doi.org/10.1137/0111030> doi: 10.1137/0111030
- Miller, R. L. (1997). Tropical thermostats and low cloud cover. *Journal of Climate*, 10(3), 409–440. doi: 10.1175/1520-0442(1997)010<0409:TTALCC>2.0.CO;2
- Myers, T. A., & Norris, J. R. (2016, March). Reducing the uncertainty in subtropical cloud feedback. *Geophysical Research Letters*, 43(5), 2144–2148. Retrieved from <https://doi.org/10.1002/2015gl067416> doi: 10.1002/2015gl067416
- Myers, T. A., Scott, R. C., Zelinka, M. D., Klein, S. A., Norris, J. R., & Caldwell, P. M. (2021). Observational constraints on low cloud feedback reduce uncertainty of climate sensitivity. *Nature Climate Change*, 11(6), 501–507. Retrieved from <http://dx.doi.org/10.1038/s41558-021-01039-0> doi: 10.1038/s41558-021-01039-0
- Norris, J. R., & Iacobellis, S. F. (2005, November). North pacific cloud feedbacks inferred from synoptic-scale dynamic and thermodynamic relationships. *Journal of Climate*, 18(22), 4862–4878. Retrieved from <https://doi.org/10.1175/jcli3558.1> doi: 10.1175/jcli3558.1
- Norris, J. R., & Weaver, C. P. (2001). Improved techniques for evaluating GCM cloudiness applied to the NCAR CCM3. *Journal of Climate*, 14(12), 2540–2550. doi: 10.1175/1520-0442(2001)014<2540:ITFEGC>2.0.CO;2
- North, G., & Kim, K.-Y. (2017). *Energy balance climate models*. Weinheim, Germany: Wiley-VCH.
- Peters, M. E., & Bretherton, C. S. (2005). A simplified model of the Walker circulation with an interactive ocean mixed layer and cloud-radiative feedbacks. *Journal of Climate*, 18(20), 4216–4234. doi: 10.1175/JCLI3534.1
- Pierrehumbert. (1995, may). Thermostats, Radiator Fins, and the Local Runaway Greenhouse. *Journal of the Atmospheric Sciences*, 52(10), 1784–1806. Retrieved from [http://journals.ametsoc.org/doi/10.1175/1520-0469\(1995\)052%3C1784:TRFATL%3E2.0.CO;2](http://journals.ametsoc.org/doi/10.1175/1520-0469(1995)052%3C1784:TRFATL%3E2.0.CO;2) doi: 10.1175/1520-0469(1995)052<1784:TRFATL>2.0.CO;2
- Pierrehumbert, & Swanson. (1995, jan). Baroclinic Instability. *Annual Review of Fluid Mechanics*, 27(1), 419–467. Retrieved from <http://fluid.annualreviews.org/cgi/doi/10.1146/annurev.fluid.27.1.419> doi: 10.1146/annurev.fluid.27.1.419
- Qu, X., Hall, A., Klein, S. A., & DeAngelis, A. M. (2015, September). Positive tropical marine low-cloud cover feedback inferred from cloud-controlling factors. *Geophysical Research Letters*, 42(18), 7767–7775. Retrieved from <https://doi.org/10.1002/2015gl065627> doi: 10.1002/2015gl065627
- Rutan, D. A., Kato, S., Doelling, D. R., Rose, F. G., Nguyen, L. T., Caldwell, T. E., & Loeb, N. G. (2015, June). CERES synoptic product: Methodology and validation of surface radiant flux. *Journal of Atmospheric and Oceanic Technology*, 32(6), 1121–1143. Retrieved from <https://doi.org/10.1175/jtech-d-14-00165.1> doi: 10.1175/jtech-d-14-00165.1
- Sellers, W. D. (1969, jun). A Global Climatic Model Based on the Energy

- Balance of the Earth-Atmosphere System. *Journal of Applied Meteorology*, 8(3), 392–400. Retrieved from [http://journals.ametsoc.org/doi/abs/10.1175/1520-0450\(1969\)008<0392:AGCMBO>2.0.CO;2](http://journals.ametsoc.org/doi/abs/10.1175/1520-0450(1969)008<0392:AGCMBO>2.0.CO;2) doi: 10.1175/1520-0450(1969)008<0392:AGCMBO>2.0.CO;2
- Sherwood, S. C., Webb, M. J., Annan, J. D., Armour, K. C., Forster, P. M., Hargreaves, J. C., ... Zelinka, M. D. (2020, December). An assessment of earth's climate sensitivity using multiple lines of evidence. *Rev. Geophys.*, 58(4).
- Siebesma, A. P., Bony, S., Jakob, C., & Stevens, B. (Eds.). (2020). *Clouds and climate*. Cambridge University Press. Retrieved from <https://doi.org/10.1017/9781107447738> doi: 10.1017/9781107447738
- Sobel, A. H., Nilsson, J., & Polvani, L. M. (2001). The weak temperature gradient approximation and balanced tropical moisture waves. *Journal of the Atmospheric Sciences*, 58(23), 3650–3665. doi: 10.1175/1520-0469(2001)058<3650:TWTGAA>2.0.CO;2
- Södergren, A. H., McDonald, A. J., & Bodeker, G. E. (2018). An energy balance model exploration of the impacts of interactions between surface albedo, cloud cover and water vapor on polar amplification. *Climate Dynamics*, 51(5-6), 1639–1658. Retrieved from <http://dx.doi.org/10.1007/s00382-017-3974-5> doi: 10.1007/s00382-017-3974-5
- Stephens, G. L., O'Brien, D., Webster, P. J., Pilewski, P., Kato, S., & Li, J.-I. (2015, mar). The albedo of Earth. *Reviews of Geophysics*, 53(1), 141–163. Retrieved from <http://doi.wiley.com/10.1002/2014RG000449> doi: 10.1002/2014RG000449
- Stevens, B., & Brenguier, J.-L. (2009). Cloud-controlling factors: low clouds. In J. Heintzenberg & R. J. Charlson (Eds.), *Clouds in the perturbed climate system* (chap. 8). The MIT Press. Retrieved from <https://doi.org/10.7551/mitpress/9780262012874.001.0001> doi: 10.7551/mitpress/9780262012874.001.0001
- Stevens, B., & Schwartz, S. E. (2012, May). Observing and modeling earth's energy flows. *Surveys in Geophysics*, 33(3-4), 779–816. Retrieved from <https://doi.org/10.1007/s10712-012-9184-0> doi: 10.1007/s10712-012-9184-0
- Wood, R., & Bretherton, C. S. (2006). On the relationship between stratiform low cloud cover and lower-tropospheric stability. *Journal of Climate*, 19(24), 6425–6432. doi: 10.1175/JCLI3988.1
- Zelinka, M. D., Myers, T. A., McCoy, D. T., Po-Chedley, S., Caldwell, P. M., Ceppi, P., ... Taylor, K. E. (2020, January). Causes of higher climate sensitivity in CMIP6 models. *Geophys. Res. Lett.*, 47(1).